tRNA Topography during Translocation: Steady-State and Kinetic Fluorescence Energy-Transfer Studies†

Harald Paulsen and Wolfgang Wintermeyer*

Institut für Physiologische Chemie, Physikalische Biochemie, und Zellbiologie, Ludwig-Maximilians-Universität, D 8000 München 2, Federal Republic of Germany

Received August 23, 1985; Revised Manuscript Received December 3, 1985

ABSTRACT: The distances between the anticodon loops of fluorescent $tRNA^{Phe}$ bound to the E site and to either the A or the P site of poly(U)-programmed *Escherichia coli* ribosomes were measured by fluorescence energy transfer. Donor and acceptor molecules were wybutine and proflavin, respectively, both located 3′ to the anticodon of $tRNA^{Phe}$. The anticodon loops were found to be separated by 42 ± 10 Å (A to E site) and 34 ± 8 Å (P to E site). The latter distance is much larger than the one measured between the anticodon loops of A and P site bound tRNAs [24 ± 4 Å; Paulsen, H., Robertson, J. M., & Wintermeyer, W. (1983) *J. Mol. Biol. 167*, 411–426], rendering unlikely simultaneous codon–anticodon interaction in the P and E sites. In kinetic stopped-flow measurements, the energy transfer between the anticodon loops of the tRNA molecules was followed during translocation. The transfer efficiency decreases in three steps with apparent rate constants on the order of 1, 0.1, and 0.01 s^{-1}. The fast step is ascribed to the simultaneous displacement of the deacylated $tRNA^{Phe}$ out of the P site and of the *N*-AcPhe-$tRNA^{Phe}$ from the A site to the P site. The distance between the anticodon loops does not change appreciably during this reaction. A significant separation of the two tRNAs occurs during the intermediate and the slow steps. The latter most likely represents a rearrangement of the posttranslocation complex containing both tRNA molecules. The results of the kinetic energy-transfer measurements are interpreted to mean that, during the fast step, the two tRNAs are displaced in a coordinate fashion and that, after that step, the leaving tRNA is present in some intermediate state, which is related to the E site. From this state, the tRNA may either leave the ribosome or rearrange to be bound into the E site, both reactions occurring during the intermediate step.

The translocation step of ribosomal protein elongation entails the coordinate movement of at least three components of the ribosomal complex: the peptidyl tRNA is displaced from the A to the P site, the deacylated tRNA leaves the P site, and the mRNA is shifted, relative to the ribosome, by one base triplet. During the past 20 years, a considerable number of models of translocation have been put forward. These models include structural changes of the tRNA (Woese, 1970), the ribosome (Spirin, 1969; Kaziro, 1978), or the mRNA (Hardesty, 1969) or are based on the comparison of tRNA binding affinities before and after translocation (Leder, 1973; Holschuh et al., 1981). On the other hand, there are not enough data to substantiate one or the other of these models on a molecular level (Spirin, 1983). For instance, it is not clear whether the displacements of the two tRNA molecules (release of the deacylated tRNA from the P site and displacement of the peptidyl tRNA from the A site to the P site) are coupled or whether the deacylated tRNA, by the action of elongation factor G, is released first, thus opening the way for the subsequent, spontaneous displacement of the peptidyl tRNA (Leder, 1973, Holschuh et al., 1980).

A promising way toward a mechanistical understanding of the reaction of a complex biological system is to study the topography of the system before and after the reaction and, most important, during the reaction. The pretranslocative complex has been studied in most detail (Ofengand, 1980; Hardesty et al., 1985). We have focused our interest on the arrangement of the two tRNAs relative to each other. On the basis of singlet–singlet energy-transfer measurements between fluorophores located at different parts of the tRNAs, an arrangement was favored where the planes of the two L-shaped molecules form an angle of 60 ± 30° (Paulsen et al., 1983). In the present work, we have extended these energy-transfer studies to the posttranslocative state and to kinetic measurements during translocation.

As to the posttranslocative state, it has been proposed that the exit tRNA remains bound to the E site (Rheinberger et al., 1981). Although it has been shown that at low Mg^{2+} concentration most of the leaving tRNA is found dissociated from the ribosome (Robertson et al., 1984), the possiblity of transient E site binding remains. Nothing is known about the topography of this third tRNA binding site. In particular, it is a matter of debate whether codon–anticodon interaction in the E site takes place or not (Lill et al., 1984). Therefore, we set out to determine how far the anticodon loop of E site bound tRNA is separated from that of A or P site bound tRNA.

Furthermore, we have followed the fluorescence energy-transfer between the tRNA anticodon loops during translocation in stopped-flow experiments. Previously, three steps had been resolved in stopped-flow experiments of translocation, monitored by fluorophores located in the tRNA molecules (Robertson et al., 1984; J. M. Robertson et al., unpublished data). The present kinetic experiments specifically address the question during which one of the three kinetically resolvable steps the two tRNA molecules come apart. This information appears to be crucial for the decision between the synchronous or asynchronous mechanism of translocation. The technique of time-resolved fluorescence energy-transfer mea-

†This work has been supported by the Deutsche Forschungsgemeinschaft and the Fonds der Chemischen Industrie. W.W. acknowledges a Heisenberg Fellowship from the Deutsche Forschungsgemeinschaft.

*Address correspondence to this author at the Institut für Physiologische Chemie.

0006-2960/86/0425-2749$01.50/0

surement yields a wealth of information, both kinetic and topographical, and, therefore, should be useful for kinetic studies in other complex biological systems, too.

Materials and Methods

Biochemicals. The preparation of 70S ribosomes from *Escherichia coli* MRE 600, $tRNA^{Phe}$ (charging capacity 1.4 nmol of Phe/A_{260} unit) from brewers' yeast tRNA (Boehringer, Mannheim), and $tRNA^{Phe}_{Prf37}$ (charging capacity 1.3 nmol/A_{260} unit) as well as the aminoacylation and acetylation of yeast $tRNA^{Phe}$ (1.6 nmol of *N*-Ac[^{14}C]Phe/A_{260} unit, 504 Ci/mol) have been described elsewhere (Robertson & Wintermeyer, 1981). $tRNA^{Phe}$ from *E. coli* (charging capacity 1.4 nmol/A_{260} unit, Boehringer, Mannheim) was aminoacylated and acetylated according to the procedure of Rappoport and Lapidot (1974) (1.5–1.6 nmol of *N*-ac[^{14}C]Phe/A_{260} unit, 10 Ci/mol). Poly(U) was purchased from Boehringer, Mannheim. Elongation factor G (EF-G) was isolated according to Marsh and Parmeggiani (1977) and purified to apparent homogeneity as to be described elsewhere (J. M. Robertson et al., unpublished results). Concentrations of EF-G were determined (Bradford, 1976) by using 12.9 pmol/μg as calculated from the sequence (Ovchinnikov et al., 1982). The concentrations of ribosomes and tRNAs were calculated by assuming 23 pmol/A_{260} unit and 1.75 nmol/A_{260} unit, respectively. Ribosomes were 65% active with respect to tRNA binding into P, A, and E sites (Lill et al., 1984). The remaining 35% do not bind tRNA at all; therefore, the fractional activity does not interfere with the interpretation of the results of the present study.

All experiments were carried out either in buffer A [50 mM tris(hydroxymethyl)aminomethane hydrochloride (Tris-HCl) (pH 7.6), 90 mM NH_4Cl, 50 mM KCl, 1 mM dithioerythritol (DTE), and magnesium acetate as indicated] or in buffer B [50 mM Tris-HCl (pH 7.6), 30 mM NH_4Cl, 30 mM KCl, 1 mM DTE, and magnesium acetate as indicated]. Poly(U) was always present at a final concentration of 1 A_{260} unit/mL.

tRNA–Ribosome Complexes. Pretranslocative ribosome complexes were prepared essentially according to Robertson and Wintermeyer (1981), except that the ultracentrifugation step was omitted. In the kinetic translocation experiments, the amounts of tRNA to be bound to the P or A sites were about stoichiometric to the amount of active ribosomes. Thus, the P sites of poly(U)-programmed ribosomes (0.3 μM) were filled with deacylated $tRNA^{Phe}$ (0.2 μM). In a subsequent incubation, *N*-AcPhe-$tRNA^{Phe}$ (0.2 μM) was bound to the A sites. If the magnesium concentration in the experiment was 10 mM or lower, the incubations were performed at 5-fold tRNA and ribosome concentrations in the same buffer in order to achieve higher binding efficiency. The solutions then were diluted prior to the translocation experiments. The analysis of the tRNA–ribosome complexes by trichloroacetic acid precipitation, nitrocellulose filter binding, and puromycin assays has been described elsewhere (Robertson & Wintermeyer, 1981).

Translocation. The translocation reaction was initiated by the addition of EF-G and GTP (final concentrations 0.8 μM and 0.5 mM, respectively). The EF-G was preincubated with 20 mM GTP for 5 min at 0 °C in 20 mM Tris-HCl (pH 6.5). In the kinetic experiments, EF-G and GTP were diluted to twice the final concentration in the buffer used. An 80-μL sample of this solution was then mixed in the stopped-flow apparatus (see below) with the same volume of the solution containing pretranslocative ribosome complexes. In experiments where the steady-state fluorescence before and after translocation was to be measured, the tRNA–ribosome complexes were diluted to half the concentrations given in the last section prior to the addition of EF-G and GTP in order to reach the same concentrations of complexes and factor in both kinetic and steady-state experiments.

In order to determine the time required for completion of the translocation reaction as seen by the puromycin reactivity of translocated peptidyl tRNA, a rapid puromycin assay was performed. Immediately after the translocation (100 μL, concentrations as under stopped-flow conditions) was started, puromycin (2 mM) was added, and the reaction was stopped after a 1-min incubation at 20 °C, following the standard procedure of the assay (Robertson & Wintermeyer, 1981). A total of 80%–90% of initially A site bound *N*-AcPhe-$tRNA^{Phe}$ was found to have reacted. A control experiment with ribosome complexes containing *N*-AcPhe-$tRNA^{Phe}$ in the P site revealed that the puromycin reaction under these conditions is about 90% complete after 1 min. We conclude that in the translocation experiments at least 90% of *N*-AcPhe-$tRNA^{Phe}$ have been translocated within this time interval.

Steady-State Fluorescence Measurements. Fluorescence measurements with tRNA–ribosome complexes in the steady state were made at 25 °C as described previously (Paulsen et al., 1983) by using a Schoeffel RRS 1000 fluorometer equipped with a double monochromator for excitation. The excitation wavelength was 320 nm (bandwidth 3 nm). The emitted light was passed through a cut-off filter (Schott WG 335) and scanned at a bandwidth of 3 nm. The spectra were digitized at a resolution of 0.5 nm and transferred to a Tektronix 4052 computer for evaluation. All spectra were corrected for blank spectra taken from homologous samples in which the fluorescent tRNAs were replaced by nonfluorescent tRNAs from *E. coli*.

Kinetic Measurements. Stopped-flow experiments were performed at 20 °C in an apparatus that has been described elsewhere (Wintermeyer & Robertson, 1982), except that the exciting light (311 nm) was isolated by a double monochromator. The emission of either proflavin or wybutine was measured after passage through cut-off filters (Schott KV 500 and KV 399, respectively). The fluorescence of wybutine in the presence of proflavin was detected by using a band filter [Schott SFK 20, 435 (±15) nm].

Sampling of the data and evaluation of the kinetic curves were performed as described elsewhere (Wintemeyer & Robertson, 1982). For each translocation experiment, at least 10 measurements were made, usually in several independent experiments. The errors given for the apparent reaction rates and the amplitudes have been estimated from the variation of these determinations.

Evaluation of Energy-Transfer Data. The determination of the energy-transfer efficiency E from the comparison of the donor fluorescence in the absence and in the presence of the energy acceptor as well as the calculation of the critical distances R_0 for the donor–acceptor pairs used here and of the donor–acceptor distances from E and R_0 have been described previously (Paulsen et al., 1983).

In the determination of the energy-transfer efficiency between *N*-AcPhe-$tRNA^{Phe}$ and $tRNA^{Phe}_{Prf37}$ in the A and E sites, respectively, the raw transfer efficiency E_{obsd} had to be corrected for the fractions of unbound *N*-AcPhe-$tRNA^{Phe}$ that did not participate in energy transfer and P site bound *N*-AcPhe-$tRNA^{Phe}$, which transferred its energy to E site-bound $tRNA^{Phe}_{Prf37}$ with 0.38 efficiency. The corrected transfer efficiency E is thus obtained as

$$E = E_{obsd}(c_T/c_B) - 0.38(c_P/c_T)$$

where c_T, c_B, and c_P are the total, ribosome-bound, and pu-

romycin-reactive amounts, respectively, of *N*-AcPhe-tRNA^{Phe}.

Energy-Transfer Efficiencies in Kinetic Experiments. In order to evaluate the changes of acceptor fluorescence in terms of transfer-efficiency changes, it was necessary to separate the fraction of the fluorescence signal that was due to energy-transfer-stimulated proflavin emission from the contributions of wybutine and directly excitated proflavin. The latter contribution can be measured separately by using a pretranslocative complex containing nonfluorescent *N*-AcPhe-tRNA^{Phe} from *E. coli* instead of the homologue from yeast. The signal due to the long-wavelength emission of the donor wybutine is obtained from the wybutine fluorescence intensity during the translocation experiment with energy transfer taking place. Under our measuring conditions, the wybutine fluorescence detected above 500 nm is about 30% of that measured at 435 nm.

The sensitized acceptor fluorescence I^s now is proportional to the energy-transfer efficiency E, the quantum efficiency of the acceptor q^A, and the absorbance of the donor A^D (Fairclough & Cantor, 1979a):

$$I^s \sim A^D E q^A$$

Since the initial transfer efficiency is known from steady-state measurements (Paulsen et al., 1983), the apparent energy-transfer efficiencies after the ith reaction step can be calculated as

$$E_i/E_0 = (I^s_i/I^s_0)(q^A{}_0/q^A{}_i)$$

if the absorbance of the donor A^D is assumed to remain constant throughout the reaction (the subscripts 0 and i denote the values before the reaction and after step i, respectively). The quantum efficiencies of the acceptor fluorescence can be determined from the acceptor fluorescence intensities I^A measured in the absence of the energy donor, assuming that also the absorbance of the acceptor fluorophore A^A does not change during the reaction:

$$q^A \sim I^A/A^A \qquad q^A{}_0/q^A{}_i = I^A{}_0/I^A{}_i$$

Donor–Acceptor Distances. The calculation of critical distances, R_0, and of donor–acceptor distances from energy-transfer efficiencies and R_0 values has been described in a previous paper (Paulsen et al., 1983). The fluorescence anisotropy data, on the basis of which the uncertainty range of the orientation factor κ^2 has been determined according to Dale et al. (1979), as well as the procedure for the calculation of the spectral overlap integrals and the fluorescence quantum yields, have also been described previously (Paulsen et al., 1983). The donor quantum yields used for the calculations are given in Table I. For P site bound tRNA$^{Phe}_{Prf37}$, $q^A{}_0 = 0.30$ has been used.

RESULTS

Steady-State Energy-Transfer Measurements between tRNAs Bound to the E Site and to either the A or P Site. In order to obtain some information about the topology of the E site in relation to the other two tRNA binding sites of the *E. coli* ribosome, the distances have been measured by fluorescence energy transfer between the anticodon loops of an E site bound tRNA and a tRNA bound to the A or P site. The fluorophores used, wybutine and proflavin located 3′ to the anticodon of tRNA^{Phe} from yeast, previously have proven useful for measuring the tRNA–tRNA separation between the A and P sites (Fairclough & Cantor, 1979b; Paulsen et al., 1983).

For positioning the donor and acceptor-containing tRNA molecules specifically into the desired binding sites, we took advantage of the fact that the binding constants (for yeast tRNA^{Phe}) of P, A, and E sites decrease by at least an order of magnitude in that sequence (Lill et al., 1984; R. Lill et al., unpublished results) and that the E site is not accessible for the peptidyl tRNA analogue *N*-AcPhe-tRNA^{Phe}. Since the rates of tRNA exchange in the P and A sites are low (half-times of hours) as compared to the duration of the experiments, these sites could be sequentially and completely occupied before filling the E site.

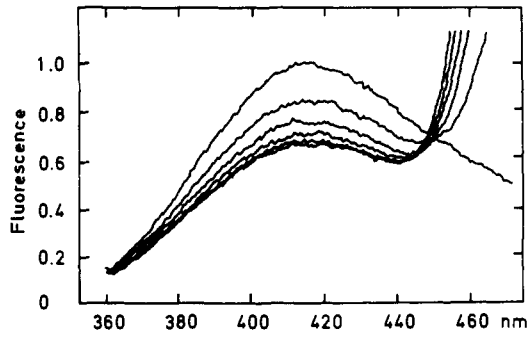

FIGURE 1: Fluorescence energy transfer between P site bound tRNA^{Phe} and E site bound tRNA$^{Phe}_{Prf37}$. Ribosome complexes containing yeast tRNA^{Phe} in the P sites and *N*-AcPhe-tRNA^{Phe} from *E. coli* in the remaining open P sites and in the A sites were prepared according to the procedure given under Materials and Methods. A total of 0.3 μM poly(U)-programmed ribosomes was incubated with 0.15 μM tRNA^{Phe} and 0.4 μM *N*-AcPhe-tRNA^{Phe} in the first and second binding reaction, respectively, in buffer A containing 20 mM Mg^{2+}. Under these conditions, virtually all added tRNA^{Phe} is bound to the P site (Lill et al., 1984). Emission spectra were measured (in the order of decreasing fluorescence intensity at 420 nm) after the addition of 0, 0.2, 0.4, 0.6, 0.8, and 1.0 μM tRNA$^{Phe}_{Prf37}$. The complexes were analyzed before and after the titration and shown to be stable for the duration of the experiment (less than 3% of A site bound *N*-AcPhe-tRNA^{Phe} exchanged). The spectra have been corrected for dilution during the titration (less than 10%) and for background fluorescence (see Materials and Methods). At saturation of the E site, a transfer efficiency $E = 0.38$ was obtained.

Thus, in order to measure the tRNA–tRNA separation between the P and E sites, the tRNA–ribosome complexes were constructed by three subsequent incubations. First, tRNA^{Phe} containing wybutine was bound into the P site of poly(U)-programmed ribosomes present in excess. Then the A sites (and the still unblocked P sites) were completely filled with an excess of nonfluorescing *N*-AcPhe-tRNA^{Phe} from *E. coli*. Finally, tRNA$^{Phe}_{Prf37}$ carrying proflavin was added, binding to the E site, the only site being still unoccupied.

It should be noted that the ribosome complexes prepared for the distance measurements differ from the posttranslocation complex in that, in addition to P and E sites, also the A sites are occupied. It is, however, unlikely that the presence of *N*-AcPhe-tRNA^{Phe} in the A site disturbs the positioning of the E site bound tRNA since the binding constant of tRNA^{Phe} in the E site is not influenced by the occupation of the A site (Wintemeyer et al., 1985).

Upon binding of tRNA$^{Phe}_{Prf37}$ to the E site, the fluorescence intensity of wybutine in the P site bound tRNA decreases as is expected because of energy transfer from wybutine to proflavin (Figure 1). The effect can be titrated by adding increasing amounts of acceptor-containing tRNA, the E site being virtually completely occupied at a 4-fold excess of tRNA$^{Phe}_{Prf37}$ over ribosomes (Figure 1). Further addition of tRNA$^{Phe}_{Prf37}$ did not influence the wybutine fluorescence any more. In a control experiment, nonfluorescent tRNA^{Phe} from *E. coli* was bound to the E site instead of tRNA$^{Phe}_{Prf37}$. There was no effect on the wybutine emission, indicating that the decrease of wybutine fluorescence intensity shown in Figure 1 is indeed due to energy transfer to proflavin.

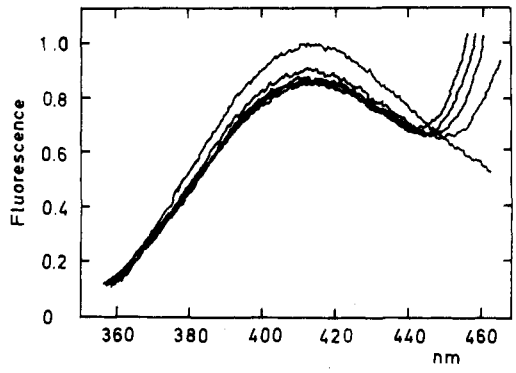

FIGURE 2: Fluorescence energy transfer from A site bound *N*-AcPhe-tRNA^{Phe} to E site bound tRNA$^{Phe}_{Prf37}$. Ribosome complexes carrying *N*-AcPhe-tRNA^{Phe} in the A site were constructed by performing the following incubations in buffer A containing 20 mM Mg^{2+} (see Materials and Methods). The P sites of poly(U)-programmed ribosomes (0.3 μM) were completely blocked by adding 0.25 μM tRNA^{Phe} from *E. coli*. Subsequently, yeast *N*-AcPhe-tRNA^{Phe} (0.12 μM) was almost quantitatively bound to the A site. Finally, the remaining open A sites were completely blocked with *N*-AcPhe-tRNA^{Phe} from *E. coli* (0.2 μM, 10 Ci/mol). The spectra were recorded (in the order of decreasing fluorescence intensity at 420 nm) after adding 0, 0.3, 0.6, 0.9, and 1.2 μM tRNA$^{Phe}_{Prf37}$. The analysis of the complexes revealed that 90% of *N*-AcPhe-tRNA^{Phe} from yeast were bound, of which 8% were puromycin-reactive. Raw transfer efficiency E_{obsd} = 0.15. Corrected transfer efficiency (see Materials and Methods) E = 0.14.

The principle of measuring the energy transfer between tRNAs bound to the A and E sites was essentially the same. *N*-AcPhe-tRNA^{Phe} containing the donor fluorophore was incubated with an excess of poly(U)-programmed ribosomes, the P site of which had been blocked with nonfluorescent tRNA from *E. coli*. After the unoccupied A sites were filled with *E. coli N*-AcPhe-tRNA^{Phe}, the E site was titrated with tRNA$^{Phe}_{Prf37}$. As shown in Figure 2, again the wybutine fluorescence was depressed, the effect approaching saturation at a ratio of tRNA$^{Phe}_{Prf37}$ to ribosomes of about 4.

In the experiment of Figure 1, each donor fluorophore was associated to a ribosomal complex containing an energy acceptor, and therefore participated in energy transfer. Thus, the difference of wybutine fluorescence measured in the absence and in the presence of a saturating amount of tRNA$^{Phe}_{Prf37}$ is a direct measure for the efficiency of energy transfer. On the other hand, in experiments where the energy transfer between A and E site bound tRNAs was to be measured (Figure 2), because of the relatively low binding constant of the A site, not all of the donor-containing *N*-AcPhe-tRNA^{Phe} was bound to the A site. Small fractions of it remained unbound or were bound to the P site. Therefore, the apparent energy-transfer efficiency had to be corrected for the fractions of donor molecules remaining unbound and therefore being inactive in energy transfer and of donor molecules bound to the P site and thus transferring energy with higher efficiency than A site-bound *N*-AcPhe-tRNA^{Phe} (Figure 1). The site location of *N*-AcPhe-tRNA^{Phe} was determined by assaying the puromycin reactivity of the complexes at the end of the experiments. At least 80% of *N*-AcPhe-tRNA^{Phe} molecules were found to be bound to the A site; hence, only a minor correction of the apparent transfer efficiencies was necessary.

From the energy-transfer efficiencies thus found, 0.38 for the transfer from the P to the E site and 0.14 for the transfer from the A to the E site, donor–acceptor distances were calculated as described previously for distance measurements between A and P site bound tRNAs (Paulsen et al., 1983). The distances are given in Table I along with the critical distances R_0 characteristic for the donor–acceptor pairs used.

Table I: Calculation of Donor–Acceptor Distances[a]

energy donor (location)	J_{DA}[b]	q_D	κ^2	R_0 (Å)	E[c]	R (Å)
tRNA^{Phe} (P site)	4.19	0.11	0.17–2.80	24–38	0.38	34 ± 8
N-AcPhe-tRNA^{Phe} (A site)	4.10	0.13	0.17–2.80	24–39	0.14	42 ± 10

[a] For the calculation of the critical distance R_0 from the overlap integral J_{DA}, the quantum efficiency of donor fluorescence q_D, and the orientation factor κ^2 and for the evaluation of the energy-transfer efficiency E in terms of donor–acceptor distance R, see Materials and Methods. κ^2 values were calculated (Dale et al., 1979) on the basis of the anisotropy values measured for wybutine in the P site (0.151 ± 0.002) and in the A site (0.154 ± 0.002) (Paulsen et al., 1982); for proflavin, the value measured for P site bound tRNA$^{Phe}_{Prf37}$ (0.334 ± 0.002; Robertson & Wintermeyer, 1981) was used. [b] × 10^{14} M^{-1} cm^{-1} nm^4. [c] Experimental error ±0.01.

The R_0 values have been calculated assuming that tRNA$^{Phe}_{Prf37}$ in the E site exhibits the same absorption spectrum and fluorescence anisotropy as has been measured with P site bound tRNA$^{Phe}_{Prf37}$. The spectroscopic properties of E site bound tRNA$^{Phe}_{Prf37}$ are difficult to measure exactly because of the rather weak tRNA binding to this site but appear to intermede the ones of P site bound and free tRNA$^{Phe}_{Prf37}$. If, alternatively, the spectroscopic properties of unbound tRNA$^{Phe}_{Prf37}$ are assumed to be valid for the E site bound tRNA, this does not significantly alter the distance calculated except for the uncertainty range (see below).

The rather wide error limits of the R_0 and R values result from the large uncertainty ranges of the orientation factor κ^2. These are due to the rather restricted mobility of the fluorophores in the complex as reflected in relatively high anisotropy values of the fluorescence of both donor and acceptor. According to Dale and Eisinger (1974), the range of κ^2 values is larger the higher the fluorescence anisotropies of donor and acceptor are. As mentioned above, for E site bound tRNA$^{Phe}_{Prf37}$ the anisotropy value bound for the P site bound tRNA was used for the calculations. This may be an overestimation. A value closer to the one of the unbound molecule would result in narrower uncertainty ranges for κ^2 and, consequently, for R. Therefore, the upper and lower error limits for the distances given, which in addition comprise the experimental error in determining the transfer efficiencies E, should be regarded as extreme uncertainty margins.

Kinetic Measurements of Energy Transfer between Ribosome-Bound tRNAs during Translocation. The steady-state energy-transfer data show that, after translocation, the distance between the anticodon loops of the tRNAs remaining bound to the P and E sites is significantly larger than the one between A and P sites. Thus, not only the dissociation of the leaving tRNA but also its transition from the P site to the E site, as well as any separation of the two tRNAs during the displacement step, is expected to be reflected in a lowering of the energy-transfer efficiency. In order to follow the topographical changes of the tRNA–ribosome complex during translocation, stopped-flow kinetic experiments were performed in which the fluorescence energy transfer was followed during translocation. The decrease of the transfer efficiency could be monitored by either the increase of the fluorescence of the donor (wybutine) or by the decrease of the fluorescence of the acceptor (proflavin). Since the proflavin fluorescence was measured with much higher accuracy, the quantitative evaluations were mainly done with the latter.

Pretranslocative complexes were formed by binding tRNA$^{Phe}_{Prf37}$ and *N*-AcPhe-tRNA^{Phe} into the P and A sites, respectively (Robertson & Wintemeyer, 1981), and translocation was started by rapidly mixing these complexes with

Table II: Changes of Energy-Transfer Efficiency during Translocation[a]

step	emission (%)[b] after the reaction steps: acceptor in the presence of donor	acceptor in the absence of donor	donor in the presence of acceptor[c]	sensitized acceptor emission	energy-transfer efficiency
initial state	171	104	11	56	0.88
fast	165	103	13	49	0.78
intermediate	142	102	18	22	0.35
slow	127	100	18	9	0.15

[a] The calculations have been performed as outlined under Materials and Methods, with the data given in Figures 3 and 4. [b] The fluorescence intensities (emission above 500 nm) are normalized to the emission of unbound $tRNA^{Phe}_{Prf37}$, arbitrarily set to 100. [c] The contribution of the donor emission has been determined in the presence of the acceptor as described under Materials and Methods.

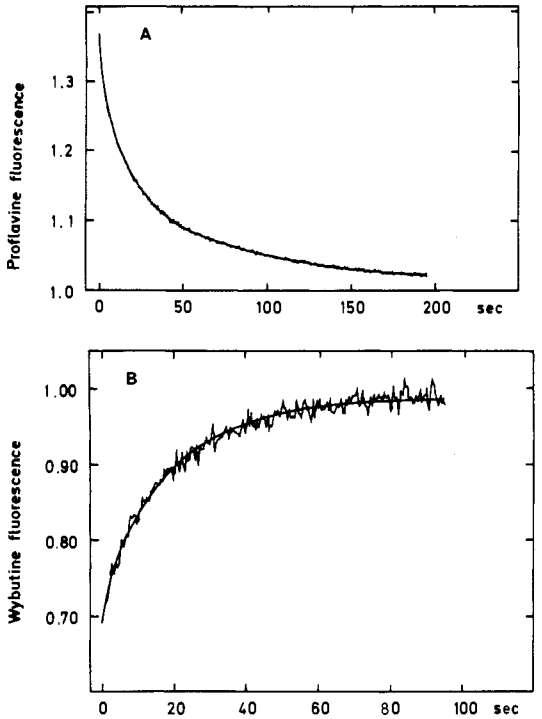

FIGURE 3: Energy transfer during translocation from *N*-AcPhe-$tRNA^{Phe}$ to $tRNA^{Phe}_{Prf37}$, initially bound to the A and P sites, respectively. (A) Emission above 500 nm, mainly due to the energy acceptor proflavin. (B) Wybutine emission at 435 nm. The experiments were performed in buffer B containing 10 mM Mg^{2+} as described under Materials and Methods. The apparent rate constants and amplitudes (relative to the final signal, corrected for the blank signal) calculated by exponential least-squares fitting (see Materials and Methods) are as follows: (A) 0.8 (±0.2) s^{-1}, 5% (±1%); 0.09 (±0.02) s^{-1}, 20% (±2%); 0.009 (±0.002) s^{-1}, 12% (±5%); (B) 0.8 (±0.2) s^{-1}, 1.1% (±0.4%); 0.09 (±0.03) s^{-1}, 3.6% (±0.4%). The smooth lines represent the functions obtained from these parameters.

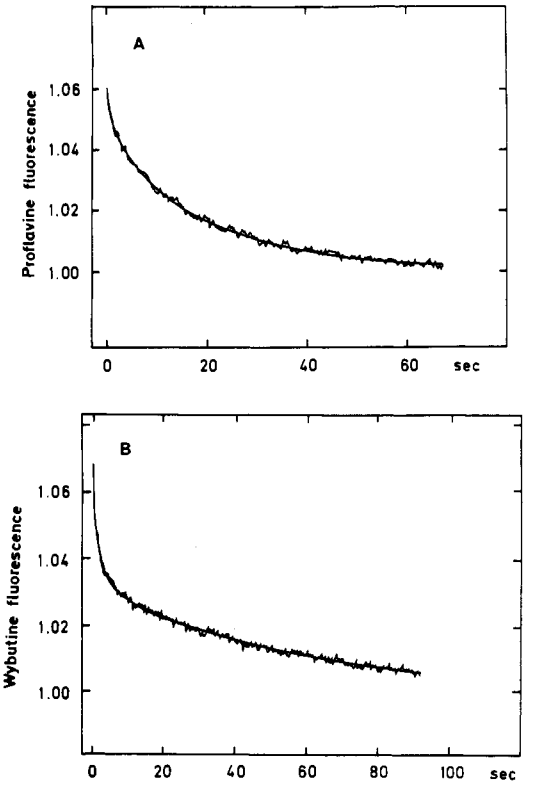

FIGURE 4: (A) Fluorescence of $tRNA^{Phe}_{Prf37}$ during the release reaction and (B) fluorescence of *N*-AcPhe-$tRNA^{Phe}$ during the displacement reaction. For the experimental conditions, see Figure 3. The tRNAs bound to the A and P sites before translocation were *N*-AcPhe-$tRNA^{Phe}$ from *E. coli* and $tRNA^{Phe}_{Prf37}$, respectively (A), and *N*-AcPhe-$tRNA^{Phe}$ from yeast and tRNA P^{he} from *E. coli*, respectively (B). The smooth lines represent the functions that have been calculated following the fitting procedure given under Materials and Methods. The apparent rates and amplitudes obtained are as follows: (A) 1.1 (±0.3) s^{-1}, 1% (±0.2%); 0.12 (±0.03) s^{-1}, 2.2% (±0.4%); 0.01 (±0.05) s^{-1}, 3% (±1%); (B) 1.7 (±0.5) s^{-1}, 2.3% (±0.5%); 0.30 (±0.10) s^{-1}, 1.7% (±0.5); 0.018 (±0.008) s^{-1}, 2.2% (±0.5%).

EF-G in the stopped-flow apparatus. Figure 3A shows that the fluorescence at the wavelength of acceptor emission decreases in at least three steps, the apparent rate constants being in the range of 1, 0.1, and 0.01 s^{-1}. For the analysis of this effect, it has to be taken into account that not only the sensitized acceptor emission but also the long-wavelength fluorescence of wybutine, as well as the emission of proflavin excited directly at the excitation wavelength of wybutine, contributes to the signal measured. In order to quantitate the signal change caused by changes of the donor or acceptor fluorescence in the absence of energy transfer, translocation experiments have been performed with homologous pretranslocative complexes except that either $tRNA^{Phe}_{Prf37}$ of *N*-AcPhe-$tRNA^{Phe}$ was exchanged with nonfluorescent $tRNA^{Phe}$ or *N*-AcPhe-$tRNA^{Phe}$, respectively, from *E. coli* (Figure 4). The fluorescence signals of the single fluorophores also change in an apparently triphasic manner similar to the one seen in Figure 3A, indicating that the signal changes represent the same three reaction steps. The amplitudes, however, are rather small as compared to the signal changes with energy transfer taking place. This means that the large decrease of fluorescence intensity seen in Figure 3A is mainly due to the energy-transfer efficiency dropping during translocation.

This conclusion is sustained by the observation that concomitantly with the depression of the acceptor emission the donor fluorescence is enhanced (Figure 3B). The time course of wybutine fluorescence has been fitted with only two apparent relaxation times, corresponding to the two faster ones derived from Figure 3A. The accuracy of the data does not suffice as to decide whether in this experiment the slowest reaction time is present.

With the knowledge of the signal changes of the fluorophores in the absence of energy transfer, the decrease of the energy-transfer-stimulated fraction of proflavin emission in

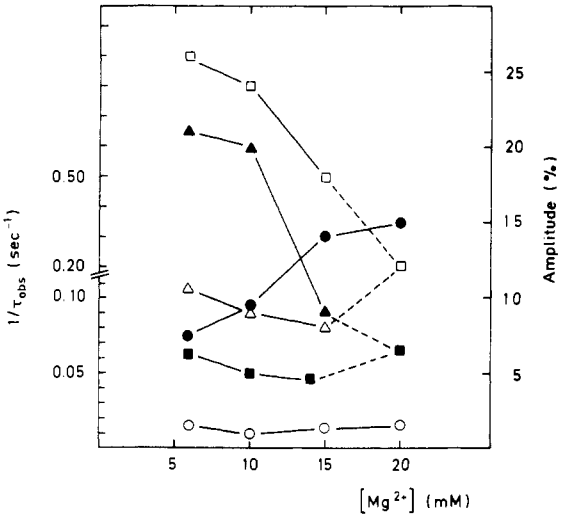

FIGURE 5: Mg^{2+} dependence of the three translocation steps as monitored by tRNA–tRNA energy transfer. Stopped-flow experiments of translocation (cf. Figure 3A) have been performed at several Mg^{2+} concentrations. The apparent rate constants (open symbols) and amplitudes (closed symbols) are given for the fast (squares), intermediate (triangles), and slow (circles) steps. Since the final fluorescence intensities in the experiments are slightly magnesium dependent (variation ±10%), the amplitudes are given relative to the final signal at 10 mM Mg^{2+}.

Figure 3A can be determined (Table II). The changes of energy-transfer efficiencies during the three steps observed, however, are not directly given by these figures, since the fraction of $tRNA^{Phe}_{Prf37}$ actually participating in energy transfer has to be quantified before. This information was taken from steady-state energy-transfer measurements performed with ribosome complexes that have been analyzed before and after translocation in order to determine the extent of translocation (Paulsen et al., 1983). After correction for the translocation efficiency (usually above 85%), the relative amplitudes of sensitized acceptor emission give the distribution of the total change of transfer efficiency between the three steps kinetically resolved (Table II).

As can be seen from Table II, the fast step exhibits the smallest amplitude of the three steps observed. The major part of the total energy-transfer change occurs during the second and third steps. The amplitude of the slow step possibly is underestimated. The $tRNA^{Phe}_{Prf37}$ released during translocation may rebind to the A site in about the same time range in which the slow step occurs (Wintermeyer & Robertson, 1982). This would lead to an increase of energy-transfer efficiency interfering with the slow decrease observed.

The slow signal change, taking several minutes for completion, is difficult to interprete in terms of functional significance. Translocation, as revealed by the puromycin assay (see Materials and Methods), has been found to be virtually complete within 1 min after the addition of EF-G (not shown). Thus, the slow step cannot belong to translocation.

In order to identify the particular step associated with the exit of deacylated tRNA, we repeated the experiment shown in Figure 3A at various Mg^{2+} concentrations. It is known that, under our experimental conditions, the exit reaction is strongly magnesium dependent (Robertson et al., 1984). At higher Mg^{2+} concentrations, more of deacylated tRNA remains bound to the E site after translocation, and therefore, the amplitude of the signal due to the exit of tRNA should be depressed. Figure 5 shows that, in fact, between 6 and 20 mM magnesium, the amplitude of the second step is depressed by a factor of 3 whereas, concomitantly, the amplitude of the slowest step significantly increases. The latter finding indicates that this step only occurs with deacylated tRNA remaining bound to the E site. Figure 5 further shows that the fast reaction is drastically slowed down with increasing magnesium concentration. Most likely, at 20 mM Mg^{2+}, the first and second steps are no longer resolved kinetically, explaining that in this experiment only two apparent steps have been found. Essentially the same results were obtained in buffer A at 15 and 20 mM Mg^{2+} (not shown).

The data shown in Figure 5 suggest that the two slower steps represent alternative reaction pathways, the usage of which can be shifted by varying the magnesium concentration. Therefore, it is not meaningful to evaluate those two energy-transfer changes in terms of distance values. On the other hand, the fast step presumably is passed by all translocating ribosome complexes present. Given the donor–acceptor distance before translocation being 23 ± 6 Å and the transfer efficiency dropping from 0.88 (Paulsen et al., 1983) to 0.78 (Table II), the fluorophores are separated by 25 ± 6 Å after this step. (The calculation has been performed as outlined under Materials and Methods assuming that the spectroscopic properties of the donor and acceptor do not change except for the fluorescence quantum yield of wybutine decreasing from 0.13 before translocation, [see Paulsen et al. (1982)] to 0.12 after the first step, see Figure 4B). These data suggest that no significant change of the distance between the two anticodon loops occurs during the fast step.

Discussion

The E site, as originally proposed by Noll et al. (1966), has been discussed to function as an exit site where deacylated tRNA is bound after translocation and before leaving the ribosome (Rheinberger & Nierhaus, 1983). For the topography of the tRNA–ribosome complex, this suggests a contiguous apposition of the three binding sites in the order A, P, and E. The distances measured between the anticodon loops of ribosome-bound tRNAs fit well into such a model, the largest separation being found between A and E sites. The three tRNAs are not necessarily straightly aligned since the E site bound tRNA does not efficiently interact with the mRNA, as discussed below, and furthermore, the mRNA may be kinked in the region of tRNA binding (Rich, 1974). In fact, the mean value of the distance between A and E sites seems to be smaller than the sum of the two other mean values, which may indicate a nonlinear arrangement of the three binding sites. However, a proper triangulation of the tRNA binding sites requires further energy-transfer experiments in order to narrow the uncertainty ranges of the distance values.

The separation of the tRNA anticodon loops in the P and E sites, 34 (±8) Å, is significantly larger than that of the tRNAs in the A and P sites, 24 (±4) Å (Paulsen et al., 1983), and most likely does not allow for simultaneous codon–anticodon interaction of the tRNAs with contiguous codons. Since codon–anticodon interaction in the P site has been shown from several lines of evidence, this means that the tRNA in the E site is not in contact with the mRNA. This conclusion rests on the assumption that the E site bound tRNA is present in a single topographically defined state. Alternatively, it is conceivable that the tRNA molecule, while it is bound to the E site, may adopt several conformational states on its way from the P site bound to the E site bound or the unbound state, and that the codon–anticodon interaction does not take place in all of these states. Different states of the ribosome may be involved as well. At any rate, however, the observed low energy-transfer efficiency, representing an average of all these states, would allow only a small fraction of the E site bound

tRNA to interact with the mRNA. This conclusion is corroborated by the finding that tRNA binding into the E site is not dependent on the presence of the cognate codon (Grajevskaja et al., 1982; Kirillov et al., 1983; Lill et al., 1984) and argues against the proposal that the E site bound tRNA is functionally important for fixing the mRNA in the correct position (Rheinberger et al., 1983).

On the basis of the steady-state results, the kinetically resolved energy-transfer changes can be interpreted in terms of the changes of the tRNA topography taking place during translocation. The interpretation rests on the assignment of the fast step to the displacement of the tRNAs. The assignment is based on separate kinetic studies of the release and displacement reactions (Robertson et al., 1984; J. Robertson, et al., unpublished results) and of the GTP hydrolysis accompanying translocation (J. Robertson, unpublished results). The main finding of these studies, which will be published in detail elsewhere, is that each of the three partial reactions of translocation gives rise to a step characterized by an apparent first-order rate constant between 1.5 and 5 s^{-1} (at 20 °C). Furthermore, it could be shown that the rate of GTP hydrolysis is limited by the displacement of the peptidyl tRNA from the A site. These results suggest that the three reactions are coupled and that the displacement of the tRNAs takes place during the fast step.

In the present kinetic energy-transfer experiments, an apparent first-order rate constant of about 1 s^{-1} has been obtained for the first step of translocation. The value is similar to the rate constants of the first resolved steps of the release and displacement reactions, mentioned above. After this step, the distance between the anticodon loops of the two tRNAs, taking part in the translocation reaction, has not changed significantly. Given the above assignment of the fast step to the displacement of the tRNAs, this result suggests that the two tRNAs are displaced simultaneously. Thus, the kinetic data do not support a model in which the EF-G-induced release of the deacylated tRNA from the P site takes place before the displacement of the peptidyl tRNA to the P site (Leder, 1973; Holschuh et al., 1981). It should be added, though, that the model cannot be excluded on the basis of kinetic data alone, since the coupled reaction cannot be distinguished from the uncoupled one in which the rate-limiting exit from the P site is followed by a fast displacement reaction.

The steady-state experiments have shown that the distance between the anticodon loops of E and P site bound tRNAs is significantly larger than the one of P and A site bound tRNAs. Thus, after the fast step, the leaving tRNA is not yet present in the E site bound state, as seen in the steady state. Rather, the tRNA is bound in an intermediate state, which probably is related to the E site.

A significant disruption of the two tRNA molecules appears to be associated with the intermediate step, during which the major part of the total signal change occurs. The amplitude of this step decreases markedly with increasing Mg^{2+} concentration. A very similar magnesium dependence has been found for the exit of deacylated tRNA from the ribosome complex after translocation: with increasing Mg^{2+} concentrations less of the tRNA dissociates from the ribosome (Robertson et al., 1984). Therefore, it is reasonable to ascribe to this step the release of the deacylated tRNA molecule. In parallel, some rearrangement to the E site bound state, which also leads to a drop of the energy-transfer efficiency, may take place.

The amplitude of the slow step exhibits a magnesium dependence inverse to the one found for the intermediate step. This suggests that the two steps represent alternative reaction pathways. Since the slow step is seen not only in tRNA–tRNA energy transfer but also in the emission of either one of the single fluorescent tRNAs, we suppose that it represents a slow conformational change of the two tRNAs or the ribosome or both.

The observation that there is no dissociation of tRNA from the ribosome during the displacement step of translocation shows that the two reactions are not coupled, implying the intermediate binding of the leaving tRNA to the E site of a related site. Thus, the present results lend general support to a three-site model of the elongation cycle proposed recently (Rheinberger & Nierhaus, 1983). It should be stressed, however, that the transient, weak E site binding reported here differs considerably from the stable, codon-dependent E site binding reported by these authors. Furthermore, the physiological significance of the intermediate binding into the E site is not yet clear.

Relative to the maximum rate of polyphenylalanine synthesis measured for our system in vitro, 5 s^{-1} (20 °C), the rate constants observed for the isolated translocation reaction are too slow. Recent preliminary data indicate that the difference is mainly due to a slower rate of translocation exhibited by the tRNA derivatives used for the present study, $tRNA^{Phe}_{Prf37}$ and *N*-AcPhe-$tRNA^{Phe}$. In order to close the kinetic gap between the two experimental systems, translocation experiments are currently being carried out that more closely approach the conditions prevailing in the polyphenylalanine synthesis system.

In the present work, the technique of singlet–singlet energy-transfer measurements for the first time has been used for the kinetic analysis of a reaction in a stopped-flow experiment. The energy-transfer-modulated fluorescence of the energy donor or the energy acceptor as an observable in kinetic experiments offers several advantages as compared to other observables such as absorbance and fluorescence intensity or polarization of single chromophores. The most important one is that the amplitudes of the signal changes, which usually do not yield much information, in the case of energy-transfer changes can be interpreted in terms of distance changes between the fluorophores in the particular reaction steps. Furthermore, the dependence of the energy-transfer efficiency on both separation and orientation of the fluorophores makes it a highly sensitive observable, which with high probability will also report structural changes that may not show up in the signals of the single fluorophores.

References

Bradford, M. M. (1976) *Anal. Biochem. 72*, 248–254.

Dale, R. E., & Eisinger, J. (1974) *Biopolymers 13*, 1573–1605.

Dale, R. E., Eisinger, J., & Blumberg, W. E. (1979) *Biophys. J. 26*, 161–194.

Fairclough, R. H., & Cantor, C. R. (1979a) *Methods Enzymol. 48*, 347–379.

Fairclough, R. H., & Cantor, C. R. (1979b) *J. Mol. Biol. 132*, 575–586.

Grajevskaja, R. A., Ivanov, Y. V., & Saminsky, E. M. (1982) *Eur. J. Biochem. 128*, 47–52.

Hardesty, B., Culp, W., & McKeehan, W. (1969) *Cold Spring Harbor Symp. Quant. Biol. 39*, 331–334.

Hardesty, B., Odom, O. W., Rychlik, W., Robbins, D., & Deng, H. Y. (1985) in *Mechanisms of Protein Synthesis* (Bermek, E., Ed.) pp 23–39, Springer-Verlag, Berlin and Heidelberg.

Holschuh, K., Bonin, J., & Gassen, H. G. (1980) *Biochemistry 19*, 5857–5864.

Holschuh, K., Riesner, D., & Gassen, H. G. (1981) *Nature (London) 293*, 675-677.
Kaziro, Y. (1978) *Biochim. Biophys. Acta 505*, 95-127.
Kirillov, S. V., Makarov, E. M., & Semenkov, Y. P. (1983) *FEBS Lett. 157*, 91-94.
Leder, P. (1973) *Adv. Protein Chem. 27*, 213-242.
Lill, R., Robertson, J. M., & Wintermeyer, W. (1984) *Biochemistry 23*, 6710-6717.
Marsh, R. C., & Parmeggiani, A. (1977) *Biochemistry 16*, 1278-1283.
Noll, H. (1966) *Science (Washington, D.C.) 151*, 1241-1245.
Ofengand, J. (1980) in *Ribosomes: Structure, Function, and Genetics* (Chambliss, G., Craven, G. R., Davies, J., Davis, K., Kahan, L., & Nomura, M., Eds.) pp 497-529, University Park Press, Baltimore, MD.
Ovchinnikov, Y. A., Alakhov, Y. B., Bundulis, Y. P., Bundule, M. A., Dovgas, N. V., Kozlov, V. P., Motuz, L. P., & Vinokurov, L. M. (1982) *FEBS Lett. 139*, 130-135.
Paulsen, H., Robertson, J. M., & Wintermeyer, W. (1982) *Nucleic Acids Res. 10*, 2651-2663.
Paulsen, H., Robertson, J. M., & Wintermeyer, W. (1983) *J. Mol. Biol. 167*, 411-426.
Rappoport, S., & Lapidot, Y. (1974) *Methods Enzymol. 29*, 685-688.
Rheinberger, H.-J., Sternbach, H., & Nierhaus, K. H. (1981) *Proc. Natl. Acad. Sci. U.S.A. 78*, 5310-5314.
Rheinberger, H.-J., & Nierhaus, K. H. (1983) *Proc. Natl. Acad. Sci. U.S.A. 80*, 4213-4217.
Rich, A. (1974) in *Ribosomes* (Nomura, M., Tissieres, A., & Lengyel, P., Eds.) pp 871-884, Cold Spring Harbor Laboratory, Cold Spring Harbor, NY.
Robertson, J. M., & Wintermeyer, W. (1981) *J. Mol. Biol. 151*, 57-79.
Robertson, J. M., Lill, R., & Wintermeyer, W. (1984) in *Metabolism and Enzymology of Nucleic Acids* (Zelinka, J., & Balan, J., Eds.) pp 307-319, Publishing House of the Slovak Academy of Sciences, Bratislava, CSSR.
Spirin, A. (1969) *Cold Spring Harbor Symp. Quant. Biol. 39*, 197-207.
Spirin, A. (1985) *Prog. Nucleic Acid Res. Mol. Biol. 32*, 75-114.
Wintermeyer, W., & Robertson, J. M. (1982) *Biochemistry 21*, 2246-2252.
Wintermeyer, W., Lill, R., Paulsen, H., & Robertson, J. M. (1986) in *Structure, Function and Genetics of Ribosomes* (Hardesty, B., & Kramer, G., Eds.) Springer, New York (in press).
Woese, C. (1970) *Nature (London) 226*, 817-820.

Binding of *Escherichia coli* Ribosomal Protein S8 to 16S rRNA: Kinetic and Thermodynamic Characterization†

Marylène Mougel, Bernard Ehresmann, and Chantal Ehresmann*
Laboratoire de Biochimie, Institut de Biologie Moléculaire et Cellulaire du CNRS, 67084 Strasbourg Cédex, France
Received June 17, 1985; Revised Manuscript Received December 18, 1985

ABSTRACT: A sensitive membrane filter assay has been used to examine the kinetic and equilibrium properties of the interactions between *Escherichia coli* ribosomal protein S8 and 16S rRNA. In standard conditions (0 °C, pH 7.5, 20 mM Mg^{2+}, 0.35 M KCl) the apparent association constant is $5 \pm 0.5 \times 10^7$ M^{-1}. The interaction is highly specific, and the kinetics of the reaction are consistent with the apparent association constant. Nevertheless, the rate of association is somewhat slower than that expected for a diffusion-controlled reaction, suggesting some steric constraint. The association is only slightly affected by temperature (ΔH = −1.8 kcal/mol). The entropy change [ΔS = +29 cal/(mol K)] is clearly the main driving force for the reaction. The salt dependence of K_a reveals that five ions are released upon binding at pH 7.5 and in the presence of 10 mM magnesium. The substitution of various anions for Cl^- has an appreciable effect on the magnitude of K_a, following the order $CH_3COO^- > Cl^- > Br^-$, thus indicating the existence of anion binding site(s) on S8. An equal number of ions were released when Cl^- was replaced by CH_3COO^-, but the absence of anion release upon binding cannot be excluded. On the other hand, the free energy of binding appears not to be exclusively electrostatic in nature. The effect of pH on both temperature and ionic strength dependence of K_a has been examined. It appears that protonation of residue(s) (with $pK \simeq 9$) increases the affinity via a generalized charge effect. On the other hand, deprotonation of some residue(s) with a $pK \simeq 5$–6 seems to be required for binding. Furthermore, the unique cysteine present in S8 was shown to be essential for binding.

The interactions between RNAs and proteins play an essential role at most levels of gene expression in the cell. However, the comprehension of the molecular mechanisms of recognition and interactions remains a crucial problem. The ribosomal machinery, which decodes the message into proteins, is itself a highly complex multimolecular assembly of several RNAs and proteins and offers possibilities to study in detail the mechanisms of RNA–protein association. In the ribosome, primary binding proteins are of particular interest. They directly interact with ribosomal RNAs and are especially important in ribosome assembly and presumably in stabilizing structural domains. Some of them are even involved in the feedback translational regulation of groups of ribosomal

† This work was supported by the Centre National de la Recherche Scientifique and the Délégation à la Recherche Scientifique et Technique.

0006-2960/86/0425-2756$01.50/0